Deep Mining 2024 – P Andrieux & D Cumming-Potvin (eds)

doi:10.36487/ACG_repo/2465_64

Evolution of fault-related seismic behaviour at Nickel Rim South Mine

Brad Simser [a], Pranay Yadav [a,*], Tony Butler [b]

[a] *Glencore Sudbury Integrated Nickel Operations, Canada*

[b] *ESG Solutions, Canada*

Abstract

The majority of the larger seismic events (above MW2.0) occurring at Glencore's Nickel Rim South Mine can be attributed to fault slip. In the mine's history, 21 larger seismic events have been recorded, and 20 of them locate in proximity to known geological structures. The damage from these events is highly variable, and the intensity and extent of the observed damage can be attributed to the energy radiation pattern, local stress conditions and incapability of installed ground support. This paper describes general seismic observations, emphasising the larger-magnitude fault-slip events. These seismic events have a significant areal extent, which in turn guides the mine's multi-tiered risk mitigation strategy that limits exposure and utilises dynamic ground support as a last line of defence. The dense microseismic array deployed at the mine has been a key tool for understanding which faults can be classified as 'seismically active' and how that activity progresses over time and mining. The smaller-magnitude seismic events help identify linear/planar trends away from stoping areas. In some cases, evident fault trends extending well below the mining horizons or deep into the footwall or hanging wall were observed well before the large seismic events associated with these structures occurred. Some examples of these trends are presented, along with discussions on how the precursory trends can be used to support and inform the mining strategy.

Although the mine's seismic risk management strategy has been very effective, there are still rockburst occurrences with varying degrees of warning and overall complex behaviour. In the cases described, no injuries occurred and the overall safety record of the mine has been excellent. This paper provides insights from an operational perspective. Further research is required to improve fault-slip forecasting and to develop risk-mitigation strategies. Some thoughts on potential areas of interest and suggested focus are given in the conclusion section.

Keywords: *fault-slip seismicity, rockburst damage, seismic monitoring, seismic risk management*

1 Introduction

Glencores' Nickel Rim South Mine (NRS) is located along the eastern limb of the Sudbury Igneous Complex (SIC), 2.6 km north of the Sudbury Regional Airport. The mine produces nickel, copper and precious metals from several zones using blasthole open stoping with cemented tailings backfill. The first stope was mined in May 2009, with the bulk of the pre-production development occurring between 2007 and 2009. The historic annual production was 1.2 M tonnes, with the current overall extraction ratio of greater than 95% as of March 2024.

Mining depths are between 1,105 and 1,720 m below surface. Hard igneous host rocks and an abundance of small-scale faults and structures have led to relatively high levels of mining-induced seismicity. The large amount of microseismicity recorded is a function of the dense array of uniaxial accelerometers and triaxial geophones (Simser & Butler 2022) deployed at the mine. The system is sensitive down to below moment magnitude (MW) –2.0. Geological structures play a prominent role in the observed seismicity, as does the

* Corresponding author. Email address: pranay.ism09@gmail.com

stiffness contrast between the different rock units observed at the mine. The principal in situ stress is sub-horizontal, trending northeast roughly parallel to the long axis of the Sudbury Basin (Figure 1), with horizontal stress approximately 1.6 to 1.8 times the weight of the overburden (vertical stress).

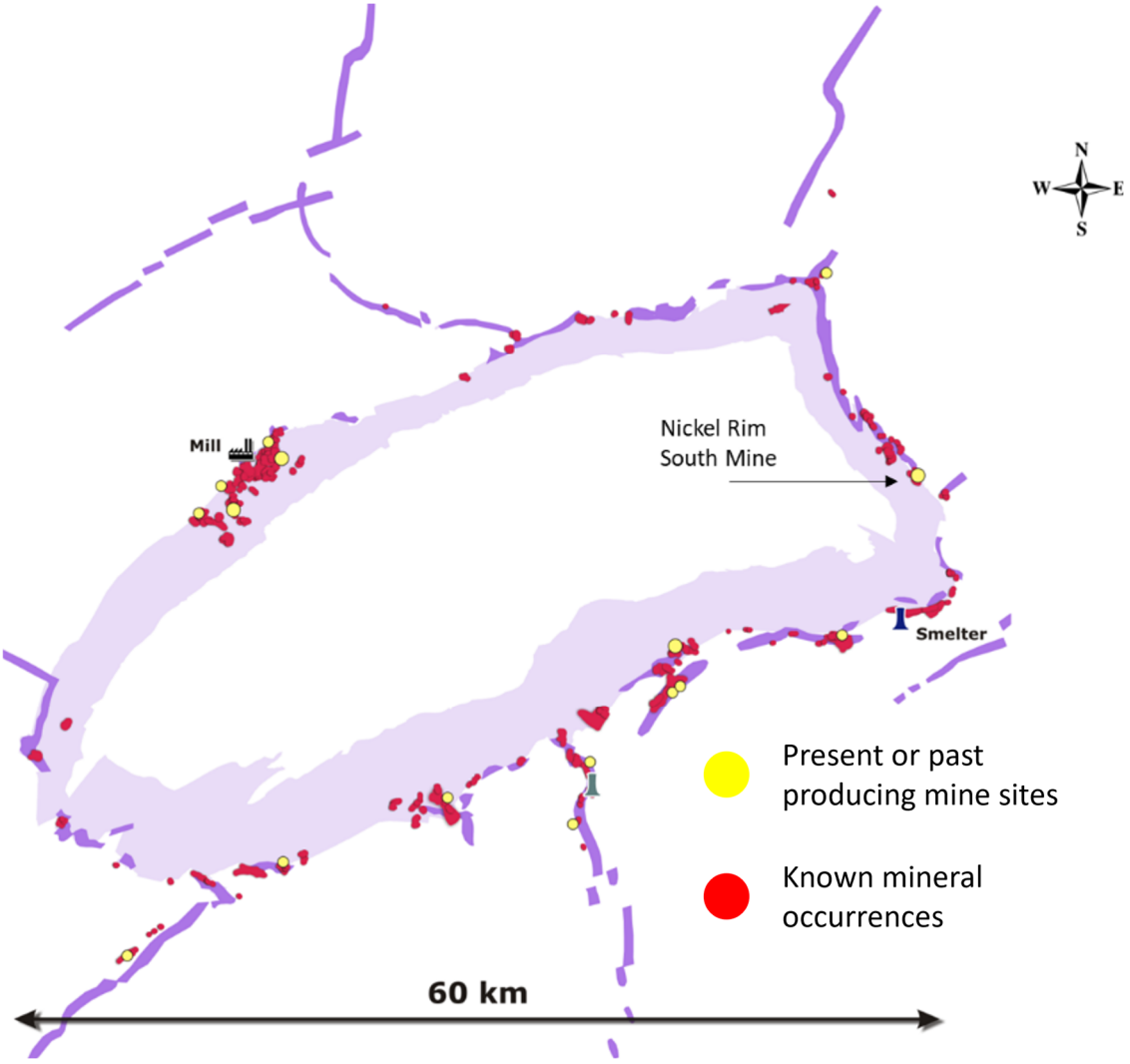

Figure 1 Simplified map of the Sudbury Basin showing the location of the mineral occurrences and the Glencore centralised mill, smelter and Nickel Rim South Mine (map shows true north)

Faulting in the mine is very complex, with some mine-scale features, but most structures are small-scale (tens to hundreds of square metres) with relatively small offsets and thickness. The large-magnitude seismicity observed at the mine is generally related to fault-slip events, typically on the mine-scale faults or more-persistent local structures. The main joint fabric (steeply dipping north–south striking jointing[1]) at the mine is subparallel to one of the main faulting trends, which can generate local small-magnitude fault-slip seismicity that possibly morphs into more significant seismic events as rock bridges between the discontinuous joints break down over time with mining. Rockbursting is generally limited to several occurrences per year but can have serious consequences. The mine utilises a multi-tiered risk-management strategy, including the widespread use of dynamic ground support, blast re-entry protocols, restricting access

[1] Note: the mine uses its own survey grid, with the mine north being 35° northeast of the true north. The mine grid north is used in the paper. For example, the principal stress direction is 20° northeast to the mine north (i.e. 55° northeast of the true north).

to older areas, remotely operated mining equipment, and a heavy emphasis on mine sequencing to minimise unfavourable mining geometries and stress conditions (Jalbout & Simser 2014).

2 Large-magnitude fault-slip seismicity

Between January 2009 and April 2024, 21 seismic events greater than MW2.0 have been recorded at the mine (Figure 2a). Twenty of these 21 larger seismic events can be related to known faulting with hypocentre locations within 20 m of a known fault and seven events within 20 m of several known faults. The largest recorded seismic event in the mine's history was MW2.9 on 3 September 2017, which occurred 18 hours following a production blast in the contact[2] zone. The large seismic event occurred along a steeply dipping north–south striking fault, with most of the aftershocks and associated damage occurring along an oblique fault that splays from the north–south structural fabric. This section focuses on the larger seismic events to highlight the fact that they tend to be related to known faulting and provides some insight into the trigger mechanisms and event characteristics.

Fault-slip seismic events tend to increase over time as more and more mining voids pierce the structure. For example, mining started in 2009; however, the first event greater than MW2.0 occurred in 2016 at approximately 50% overall extraction. As shown in Figure 2b, a considerable jump in the frequency of the larger-magnitude seismic events was observed in 2019, which was associated with mining the west abutment of the heavily extracted footwall zone, mobilising small-scale structures and daylighting the NW #2 fault along the west abutment of the contact zone. Between 2020 and 2023, a relatively consistent rate of three seismic events/year above MW2.0 was observed, and the frequency is expected to drop as the mine ramps down production in 2024.

Fault-slip events can occur at any time. It has been observed that faults tend to creep aseismically and adjust to the mining-induced stress changes more gradually than stress-fracturing events. However, a relatively large proportion (67%) of the larger seismic events at the NRS Mine have occurred within the blasting window and show a cause-and-effect relationship with the blasting activities (Figure 2c). This behaviour of fault-slip seismicity is preferable from a safety and exposure-management perspective. Central blasting (when no one is underground) captures a significant proportion of the larger events, and re-entry protocols with an extensive exclusion zone accounting for the spatial extent of known seismically active faults minimise potential workforce exposure in periods of high seismic activity.

In the large event dataset, 71% of the larger seismic events were triggered by production and 10% by development blasts. Typically, blasting activities result in local stress changes around the opening being created, and the stress-fracturing process primarily drives the observed seismicity that may vary based on the rock mass characteristics, stress conditions and the size of the opening. However, in critically loaded systems, such as stress channelling between a fault zone and an abutment of a heavily extracted mining zone, small stress changes, such as from development blasting, can trigger fault-slip events. There have been instances of delayed seismic response to blasting, with two events occurring outside of the blasting window but within 12 hours and one event within 24 hours of blasting (Figure 2d). The mine has also experienced four 'out-of-the-blue' (rogue) events that were not directly linked to any immediate blasting activities in the area. In these cases, it is possible that the longer-term stress perturbation due to mining over time was involved in generating the conditions that led to these events.

The ratio of the S-wave phase energy to the P-wave phase energy (Es/Ep) is a relatively simple method to estimate the source mechanism (van Aswegen & Butler 1993). Ratios greater than 10 are generally considered to be fault-slip events. This parameter is not 100% robust for many reasons (Morkel et al. 2019), but at a quick glance, it can provide some insight into possible event mechanisms. For example, in the large-event dataset, 62% of the events had an Es/Ep ratio of 10 or more (Figure 3a), whereas 95% occurred

[2] Contact zones in the Sudbury Basin context are nickel massive sulphide deposits, while footwall zones are copper vein type deposits.

close to known fault(s). Compared to all mine events, the large-event dataset's cumulative distribution function (CDF) shifts towards the right (Figure 3b), which is typical for a fault-slip-dominant population.

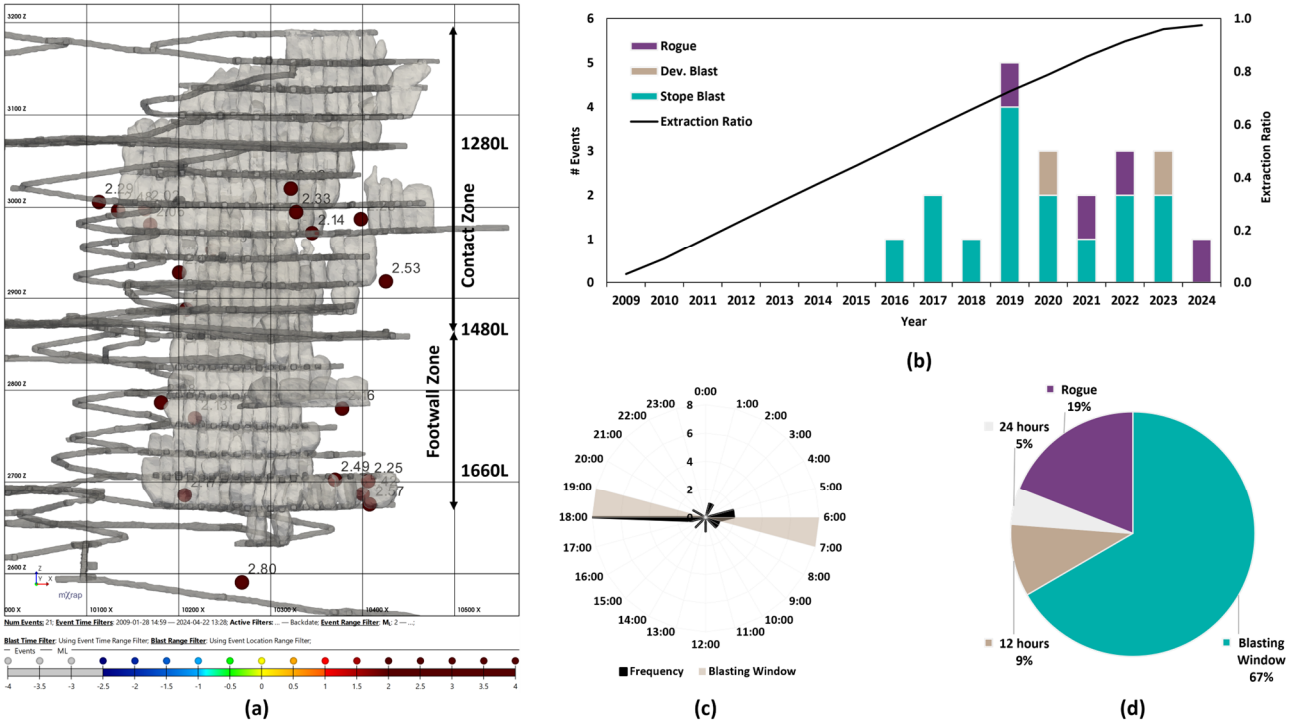

Figure 2 Summary of the 21 larger-magnitude seismic events of MW > 2.0. (a) Long section showing event locations; (b) Yearly event rate (by trigger mechanism) and extraction ratio; (c) Time of day plot; (d) Time after trigger plot

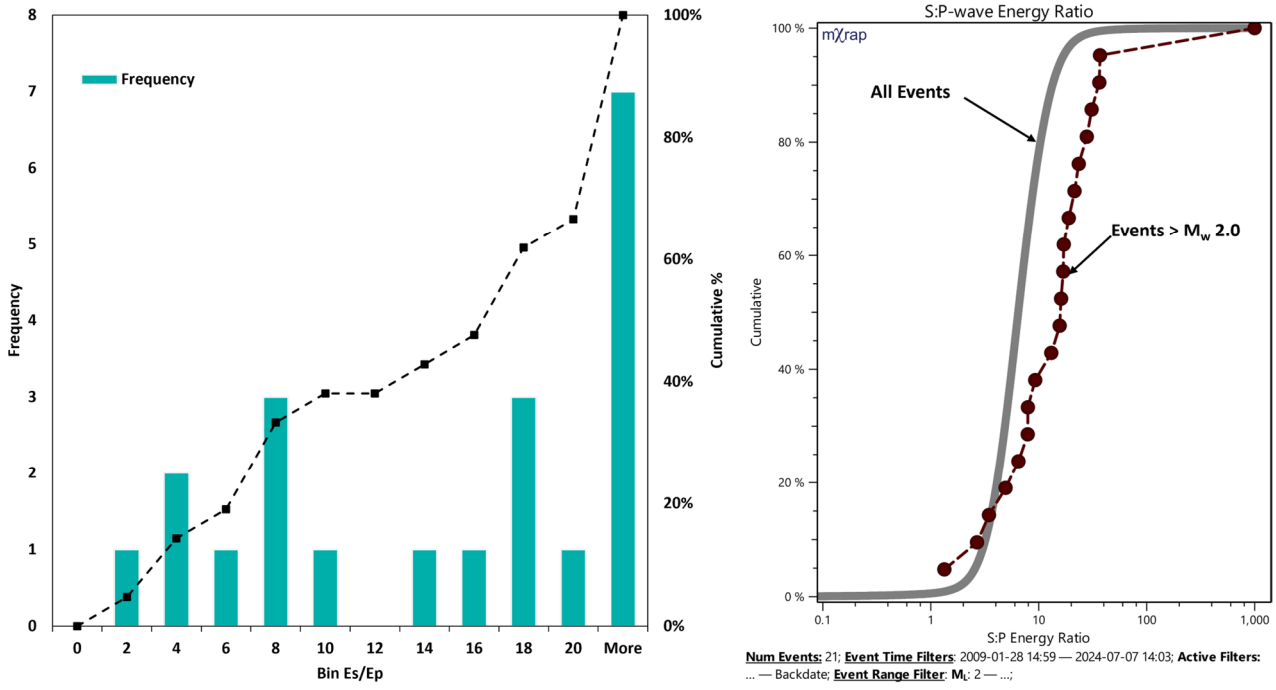

Figure 3 Es/Ep distribution for 21 larger-magnitude seismic events. (a) Histogram with cumulative percentage for Es/Ep bins; (b) Cumulative distribution function showing comparison with all mine events

Fault slip can occur in many ways, ranging from a stiff rupture of a hard patch (asperity) to a more deformation-rich large-areal slip. Although fault-slip events tend to have high Es/Ep ratios, there is no physical reason for low-ratio seismic events to be excluded from the fault-slip class of events. Asperities can form in numerous ways, such as geometric rolls, low gouge thickness areas, younger faults offsetting the older faults, crack-tip propagation where faults truncate, and rock bridges between subparallel intermediate structures, effectively creating a more throughgoing structure if the bridge ruptures, and any of these asperities could easily cause a relatively stiff, violent rupture. Another complexity when differentiating seismic source mechanisms around fault zones is the fact that stress-fracturing events occur immediately adjacent to the deforming faults. As the fault deforms, either slowly (creep) or suddenly (seismic events), the rock mass near the structure will respond, often by fracturing of the intact rock. In other words, a seismic event located close to a known fault is not absolute proof that the mechanism for the event was fault slip (Simser & Butler 2022; Simser 2022). Despite these limitations, filtering seismicity for high Es/Ep events can, at times, highlight a known fault very clearly.

The larger seismic events are more challenging to locate accurately, and they tend to have higher location uncertainties. An important consideration is that these seismic events are not point sources but can involve a substantial area of fault slipping or a large volume of rock deforming, and the event location coordinates are usually the slip-initiation point. In addition to the typical seismic system and data processing limitations such as location error, velocity models and location algorithms, the larger events often show very complex waveforms where pre-arrivals from a smaller slip can be seen before the larger slip occurs. Eight out of 21 larger events in the dataset occurred concurrently with the blast sequence, and the observed event waveforms were polluted by the blast noise, resulting in higher location uncertainty and unstable locations.

3 Damage from fault-slip seismicity

The observed rockburst damage from the fault-slip events is heavily related to its proximity to the mine openings. Rockburst incidents have occurred with smaller-magnitude events, again with proximity to the openings being a major controlling aspect, as well as other site condition factors such as installed ground support and local stress accumulation (Simser 2019). In NRS Mine's history, 48% of the larger seismic events did not result in any observable damage, and 33% had relatively minor damage. Four events (19%) had significant damage; however, over 90% of the damage in these instances occurred in areas with legacy shotcrete and rebar support that had minimal dynamic support capacity and was unable to withstand the dynamic loading during the fault-slip events. The legacy shotcrete support refers to in-cycle shotcrete and resin-grouted rebars. Currently, #4 gauge screen (5.7 mm wires with 100 mm aperture) and dynamic bolts are used in areas anticipated to experience dynamic loading. The majority of the observed damage from the larger-magnitude seismic events occurred in the events' source region (Yadav 2024). No injuries occurred in these incidents – a tribute to the seismic risk management plan in place at the mine, including central blasting, re-entry protocols, dynamic ground support, and the use of remotely operated equipment.

The triggered fault-slip episodes often show seismic activity trending along the fault zone for significant distances from the trigger (blast) location, and the large event can occur anywhere along the activated section of the fault zone due to variable fault characteristics and other contributing factors such as mobilised fault area, geometrical anomalies in the fault zone, locally stored energy around the openings, locations of asperities, fault intersections and passive sections of the fault zone due to mining or previous seismicity. This is an essential aspect of understanding the spatial influence of fault-slip seismicity that, in turn, guides the proactive seismic closures around seismically active faults. An example of these types of responses is provided in Figure 4. The NW #2 fault obliquely crosses the mine, so in effect, a portion of the fault is always impacted by elevated abutment stresses. This fault accounts for 38% of the larger seismic events in the dataset. The post-blast seismic responses of the three most intense seismic episodes in the west abutment of the contact zone provided in Figure 4a show fault activation to significant distances from the blast location along the fault zone, and the observed seismicity was associated with several delayed large events (Figure 4b). The mining geometries at the time resulted in the stress-channelling effect between the mining front and the fault zone, and the larger events and the associated damage occurred at distances greater than 100 m from the blast location (Figures 4c and 4d), highlighting the

fact that there can be a large spatial influence when the fault is triggered. The production blasts shown in Figure 4a were within 10 m of the fault zone.

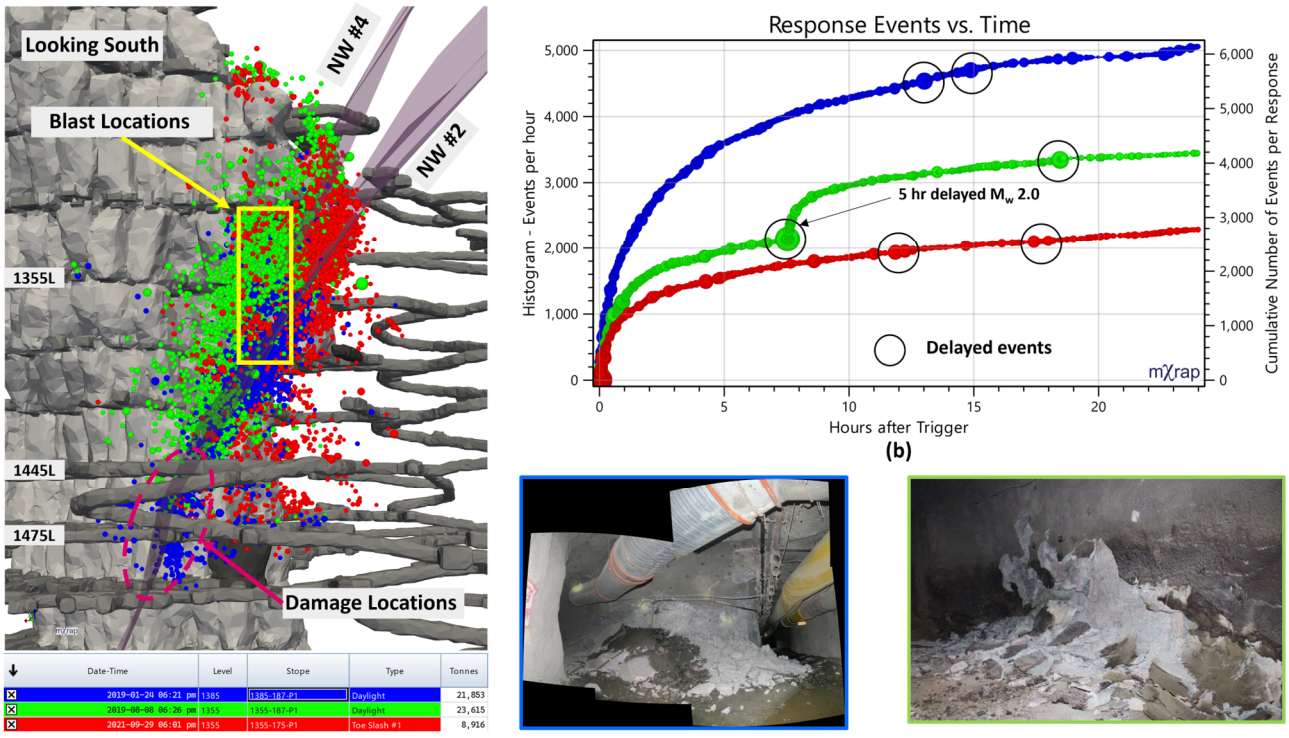

Figure 4 Post-blast (24 hours, 120 m) seismic response in the west abutment of the contact zone showing the extent of NW #2 fault activation. (a) Recorded seismicity coloured by the trigger (blast); (b) Cumulative event count for individual blasts; (c) Observed damage in the 1475-219 Orepass in January 2019, 119 m away from the blast location; (d) Observed damage in the 1445-1475 Footwall Ramp in August 2019, 161 m away from the blast location

4 Risk evolution with mining and time

The interaction between faults and mining is typically a complex evolution with varying amounts of seismic activity highly dependent on local mining proximity to the structure and overall extraction. Identifying seismically active faults is a key component of managing fault-slip seismicity. The severity of these structures can then be used to drive and support strategic and tactical mining decisions, including sequencing, excavation designs, pillar dimensions, ground support, and rate of extraction. A reliable structural model is critical for this process. The mine routinely investigates and classifies seismically active faults based on seismic monitoring, historical experience, previous instances of seismicity and damage, and the spatial extent of seismic response from blasting activities.

Seismic events that locate far from mining voids are more likely shear-type events (van Aswegen 2013). The dense seismic array deployed at the NRS Mine provides the ability to record the smaller-magnitude events that are critical in identifying linear/planar trends away from active mining areas. The NRS dataset (2009–2024) filtered for location error of less than 20 m and Es/Ep of greater than 10 is provided in Figure 5. A known fault zone, i.e. 1680 West, can be clearly seen as a planar seismic trend extending well below the orebody and active mining levels. Similar trends can be found in the seismic data in other parts of the mine when smaller time steps are used (Simser & Butler 2022; Simser 2022). Observations at NRS Mine have shown that fault zones can form barriers for seismicity, and as the mining front pushes through it, the seismicity eventually jumps across, and the fault may locally become aseismic.

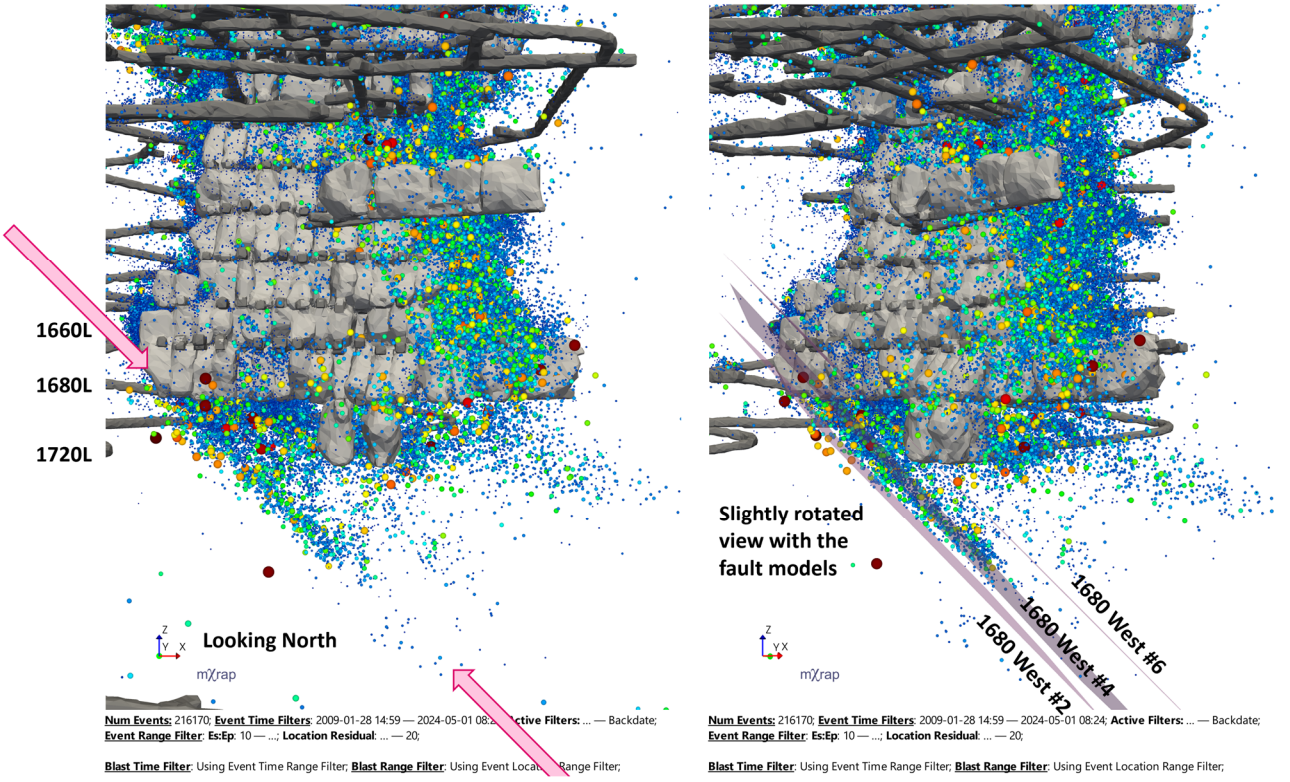

(a) (b)

Figure 5 Nickel Rim South dataset filtered for location error less than 20 m and Es/Ep greater than 10 shows a clear planar/linear trend along the known 1680 West fault zone. (a) Seismicity and mined out stopes; (b) Slightly rotated view with the geological fault models

The 1680 West fault zone is interpreted as a moderately dipping zone of three parallel faults(i.e. #2, #4, and #6, striking northwest, with #6 bounding the hanging wall and #2 bounding the footwall). The zone is characterised by weak to moderate hematite fracture fill with relatively stronger alterations observed on the footwall side. The largest recorded event in the fault zone was MW2.8 on 4 May 2023 and is the second largest event in the mines' history. The evolution of the seismic behaviour of the 1680 West fault zone is summarised in Figure 6. The seismic data is filtered for location error of less than 20 m and the distance to the modelled fault surfaces of 15 m or less. The cumulative apparent volume (CAV) trend shown is filtered for events greater than MW–1.8 to remove the effect of local sensitivity changes in the zone.

The initial mining on the first sill level (1660) pushed through the fault zone relatively early in the mine life. This period (2009–2011) had low overall extraction, and the largest recorded event in the fault zone was MW0.1, with a relatively consistent cumulative apparent volume trend. Minor elevated seismicity was observed during the 1660-1680 ramp development through the fault zone in late 2010.

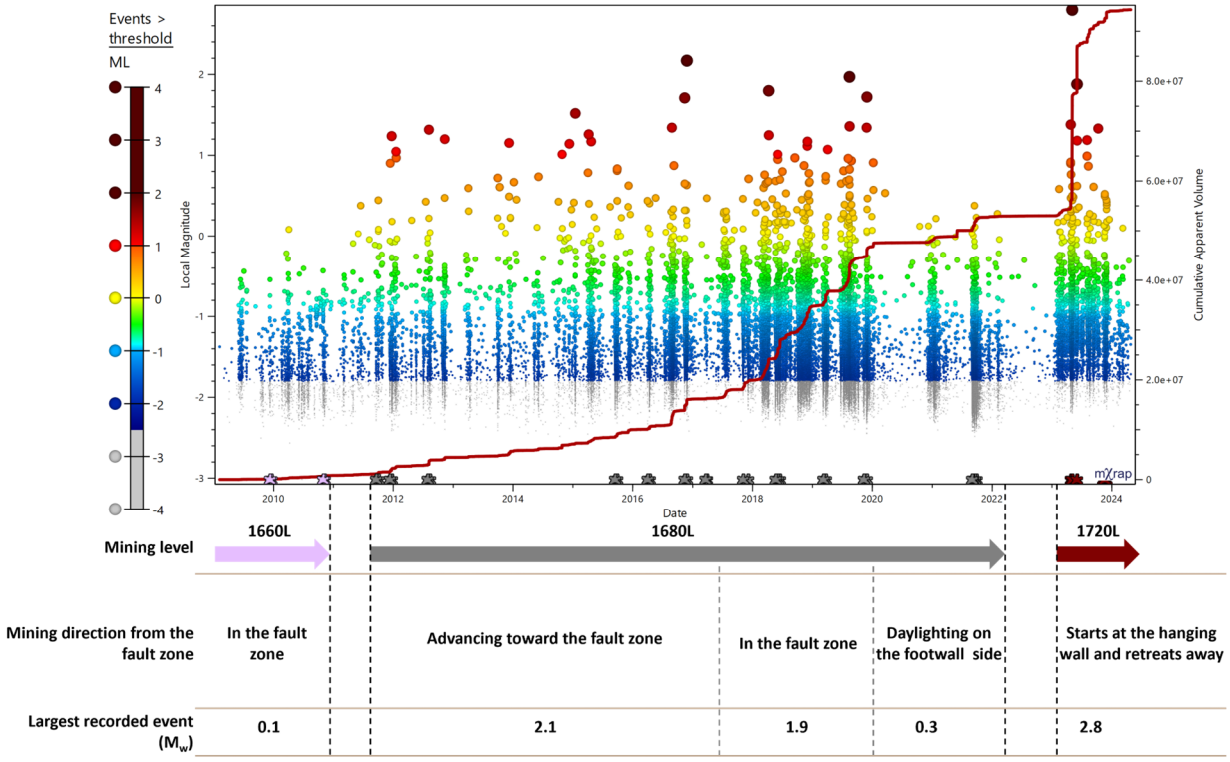

Figure 6 Magnitude–time history and cumulative apparent volume trends for the 1680 West fault zone from 2009 to 2024, showing distinct behaviours of mining around the fault zone. Relative mining direction, activities, and the largest recorded event in the respective time frames are summarised at the bottom

The first sublevel (1680) in the top-down mining sequence was extracted on a centre-out end slicing sequence, pushing the sill stresses out toward the abutments. The first stope extraction on the 1680 level showed an asymmetrical seismic response with relatively higher activity recorded along the West abutment of the stope due to the stress-channelling effect of the fault zone. The observed seismicity on this level showed three distinct behaviours based on the mining direction and distance from the fault zone. As the mining front incrementally advanced toward the fault zone (2012–2017), brittle seismic response from blasting activities was observed along the fault zone, suggesting immediate fault excitation from blasting followed by stabilisation of the driving stresses. The intensity of the observed seismicity in most cases was driven by the distance of the mining front from the hanging wall of the fault zone and the relative stress change, and it often showed a clear planar trend along the fault zone. A minor change to the CAV trend slope was observed compared to the previous time period. The stopes closer to the fault zone had an amplified stress-channelling effect and resulted in more intense seismicity. For example, the 1680-237-P1 was the first stope to pierce through the hanging wall of the fault zone in November 2016 and resulted in a MW2.1 event and a strong linear trend extending along the fault zone below active mining (Figure 7). Mining within the fault zone was associated with a substantial increase in the CAV trend, suggesting considerably higher deformation and degradation of the fault zone due to mining activities. The largest event in this time period was MW1.9 and was triggered by a development blast in August 2019 (Figure 8). Once the mining front pushed through the fault zone and daylighted on the footwall side, seismicity along the fault zone significantly reduced, and the largest recorded event in this time period was a MW0.3 (Figure 9). A challenge with fault activation is the fact that the seismic behaviour of faults evolves with increasing extraction. For example, the 1680 West fault zone in the initial years showed minor activity, and as such, a geomechanical extraction sequence to manage pillar dimensions and sill stresses was used on the first sublevel (1680) in the top-down mining sequence. As the fault behaviour became evident, limited options and flexibility were available to strategically manage fault-slip seismicity, and a tactical approach utilising dynamic ground support and re-entry protocols was used.

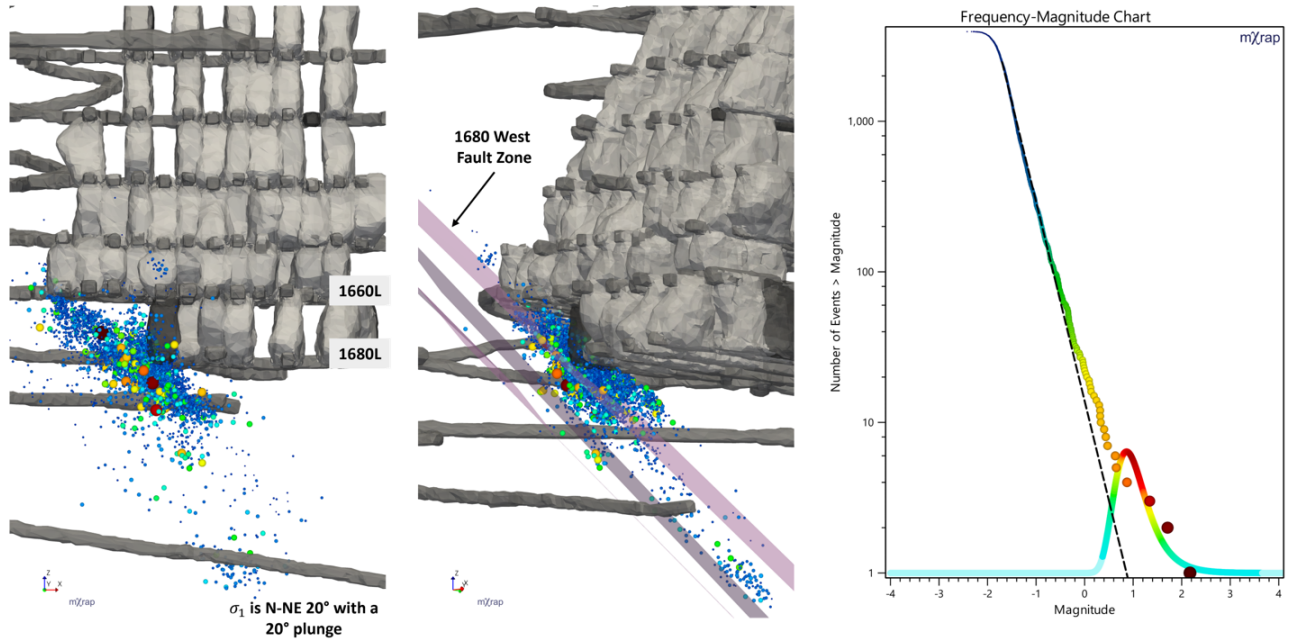

(a) (b) (c)

Figure 7 **Seismicity along the 1680 West fault zone in the year 2016 showing planar trends along the fault zone. (a) View looking north; (b) Rotated view with the fault model; (c) Frequency–magnitude relation for the event population**

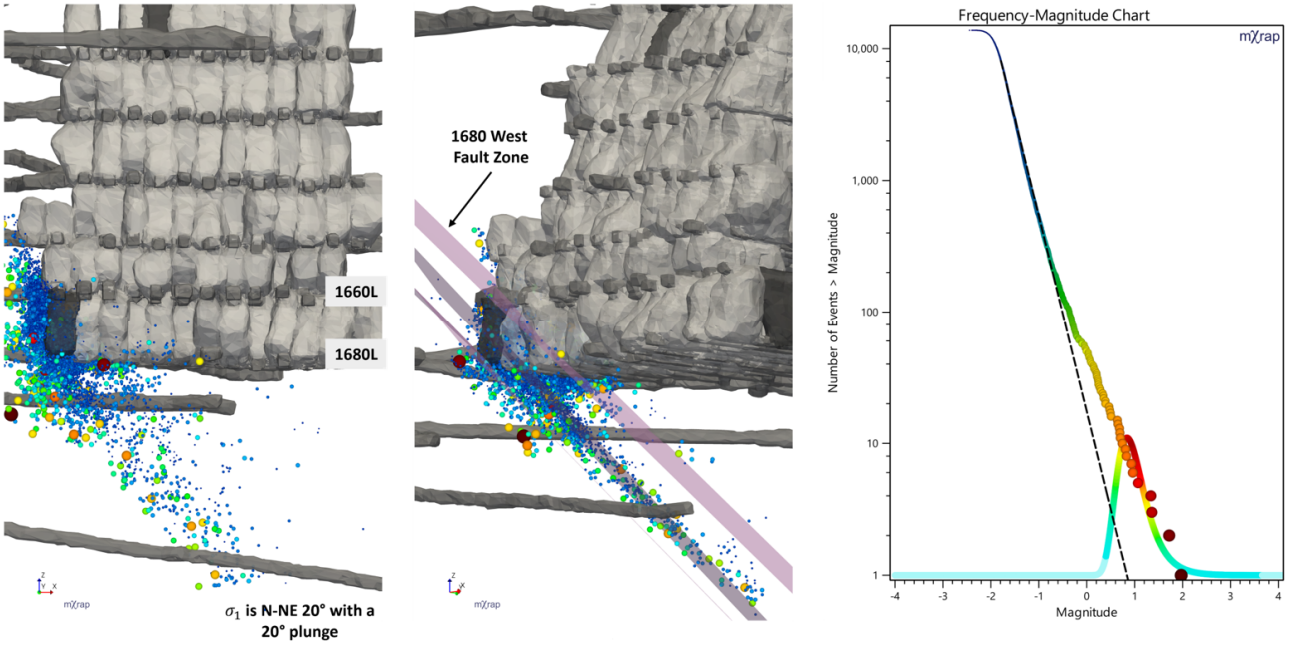

(a) (b) (c)

Figure 8 **Seismicity along the 1680 West fault zone in the year 2019 showing planar trends along the fault. (a) View looking north; (b) Rotated view with the fault model; (c) Frequency–magnitude relation for the event population**

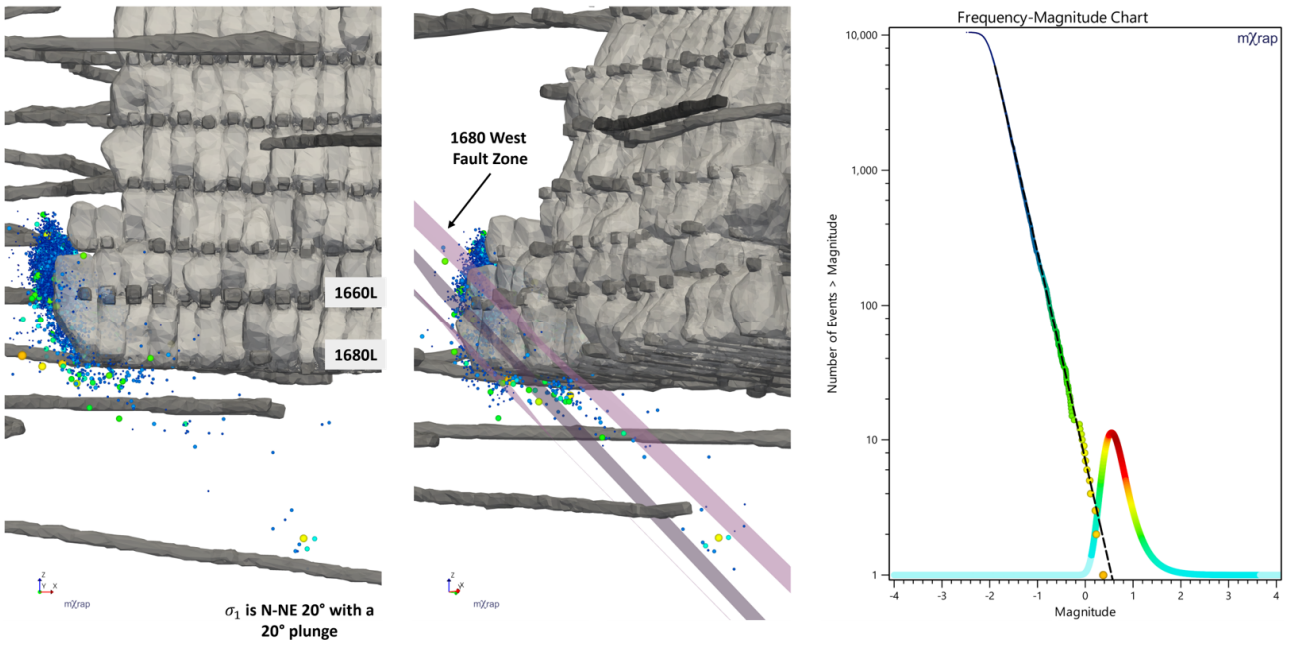

(a) (b) (c)

Figure 9 Seismicity along the 1680 West fault zone in the year 2021. Minor activity being recorded in the fault zone. (a) View looking north; (b) Rotated view with the fault model; (c) Frequency–magnitude relation for the event population

The seismic observations and experience of the fault behaviour from the first sublevel were used to inform and support the mining strategies for the next sublevel (1720) in the top-down mining sequence. Understanding the active portion of the fault zone next to the proposed mining and simulating the stress-channelling mechanisms using numerical modelling suggested that mining away from the fault zone was a more logical approach to managing the fault-slip risk. The ore extraction on the 1720 level started at the hanging wall of the fault zone and retreated away toward the east abutment. The risk-management approach was to take the relatively higher-risk stope early in the sequence instead of incrementally mining towards the fault zone and increasing the fault-slip risk. The degradation of the fault zone, with incremental mining in theory, can create a much larger area for the fault to slip. Wireless WebGen™ detonators to eliminate re-entry in the drilling horizon and allow for better blasting sequence (not shrinking pillar), enhanced ground support on the mucking horizon, and extensive and widespread re-entry protocols were used for fault-slip risk mitigation. The first stope extraction on the level resulted in a MW2.8 event with the production blast, and no observable damage occurred from the large seismic event. As the primary–secondary mining front retreated away from the fault zone, the frequency of large seismic events significantly dropped, indicating seismic hazard reduction, which is expected to continue reducing as mining progresses away from the fault zone. A few stoping lines on the west side of the leading stoping line and in the fault zone were classified as a ‘no-go’ and were removed from the mining plan, as the anticipated fault-slip risk associated with mining in the stress-trapped pillar with current and existing controls was deemed to be above the acceptable risk thresholds.

The seismic migration following a large seismic event can trigger secondary failures in other areas of the mine. Figure 10 shows the short-term (three days, 200 m) seismic response following the 4 May 2023, MW2.8 event that occurred with the second production blast on the level. An asymmetrical response was observed, with relatively higher events occurring along the west abutment of the stope due to the stress-channelling effect of the 1680 West fault zone. The seismic migration along the 1680 sill and the abutments show that a large portion of the sill instantly reacted to the fault-slip event. However, delayed responses were observed on the 1595 level along both abutments, suggesting a secondary failure process triggered by the dynamic stress wave of the large event. In this instance, the seismic migration and the secondary failure process eventually manifested in a MW1.5 seismic event and a minor strainburst in the abandoned and barricaded

200/225 crosscut on the east abutment of the 1595 level, 61 hours after and 190 m away from the MW2.8 event. This behaviour is typical for critically loaded systems, where the larger event and associated dynamic stress wave can result in a secondary failure process in other areas of the mine that were previously in a stable state, which can be instant (coiled spring) or delayed based on local site conditions such as remaining ground support capacity, stress accumulation, and structures.

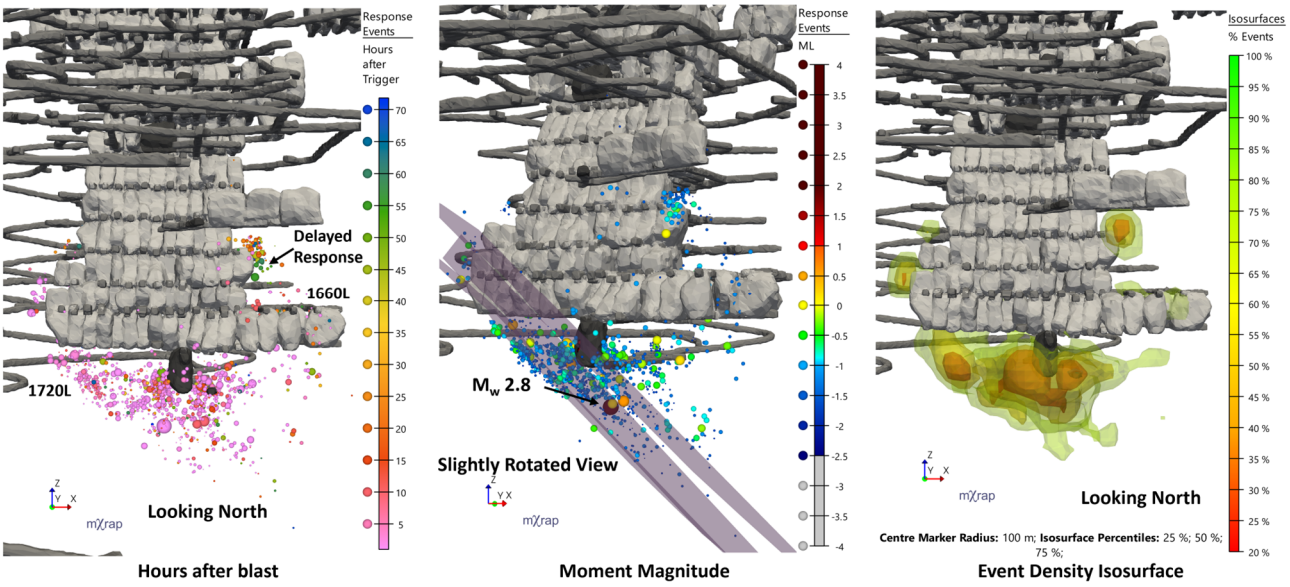

(a) (b) (c)

Figure 10 Short-term (three days, 200 m) seismic response showing the seismic migration following the MW2.8 event. Blast location is highlighted in dark grey; (a) Events by hours after the large event; (b) Events by the moment magnitude; (c) Event density isosurface of the recorded seismicity

5 Seismic moment tensor inversion

In principle, seismic moment tensor inversion (SMTI) can determine the seismic source mechanism based on the observed waveforms (Mendecki et al. 1999). However, in practice, there are numerous limiting factors and complications associated with obtaining a reliable SMTI solution for larger seismic events that are recorded by a dense seismic array, such as those experienced at NRS Mine (ESG Solutions 2021; 2022):

- waveform clipping and other near field effects
- sensor location, calibration and orientation accuracy
- sensor coverage
- sensor health and signal to noise quality
- event frequency.

The NRS Mines' underground seismic array is designed with a combination of 15 Hz geophones and 50 Hz accelerometers with the purpose of recording the smaller-magnitude, higher-frequency seismic events. The SMTI routines are often invalid for larger events due to the factors listed above. More strategically placed lower-frequency sensors would be required to adequately sample the low-frequency spectra and capture the radiation patterns from multiple directions. Events located outside of the seismic array have reduced sensor coverage on the focal sphere, and the SMTI solution is expected to have greater uncertainty. This is particularly important when analysing the source type, as a greater variation in the spectral amplitudes can introduce anomalous volumetric components to the source-type estimates (ESG Solutions 2024). The higher corner frequency events can have both arrival time and polarities impacted by wave reflection or refraction in complex mediums with sharp contrast in elastic properties such as mine voids, mine backfill, fracture zone around openings, and different lithologies (Saleh et al. 2014, 2015).

If fixed time windows are used for waveforms, this can result in early arrivals clipping and later arrivals being truncated for the larger events. Time windows can be manually lengthened from the continuous data being recorded so the full waveforms can be recaptured, but a blanket lengthening of the time window can result in other complications for data processing, such as the occurrence of multiple events in the same lengthened window. ESG Solutions is currently testing a hybrid form of dynamic trigger length detection to overcome some of the limitations that the current triggering methods impose on these monitoring systems.

A general workflow for SMTI solutions would include selecting the volume and the time span of interest, filtering the events, and using some reliability/quality index for the inversion process. Some manual spectral analysis is part of the routine to verify correct amplitudes. For example, an SMTI analysis was done for events leading up to and including the 4 May 2023, MW2.8 event along the 1680 West fault zone in the deeper part of the mine. A population of 195 events with MW greater than 0 between 2012 and 2023 were selected for the analysis. Of these seismic events, 181 had 'reliable' moment tensor inversions due to some triggers, either being significant spatial outliers or mislocated noise. The larger event (MW2.8) in the analysed dataset had a higher uncertainty along the tension (T) axis, resulting from clipped waveforms on the closer sensors and array coverage around the event location.

The SMTI results for the analysed seismic events in the 1680 West fault zone are provided in Figure 11a. The T axes suggest an upward movement toward the mine openings (Figure 11b), and the pressure (P) axes were heavily affected by the mined-out stopes, showing the compressional stress wrapping around the mine openings (Figure 11c). The stress-inversion result showed a consistent principal stress direction within 10–30° of the mines' interpreted principal stress direction. Some variation in the stress directions around seismically active fault zones is to be anticipated as the stronger faults tend to distort the stress field. This behaviour has also been observed around other faults in the mine through camera surveys of drilled blastholes and acoustic televiewer (ATV) analysis of the borehole breakouts. The borehole breakout rotations around a fault away from current mining can indicate that the fault may become problematic over time as mining-induced stresses influence the fault zone.

The poles-to-plane plot for events with less than 30% volumetric failure component shows moderately dipping failure planes that strike approximately northwest–southeast (Figure 12a). The estimated failure plane strike was in agreement with the 1680 West fault zone but was relatively shallower, and some variability was observed in estimated failure plane orientations when the results were broken down into four smaller time periods. The 1680 West fault zone is interpreted from relatively limited geological information and has low confidence in the extrapolation below the 1680 level, so some variability in the failure plane results is expected. The consistent failure mechanism through various time periods was shear with closure (Figure 12b), and the faulting type was determined to be oblique thrust (Figure 12c), where the hanging wall is moving up relative to the footwall. The likely direction of movement is intuitive as the majority of the analysed events occurred below the orebody where the fault was clamped from the sill stresses, and the upward movement toward the mine openings is likely the most favourable direction for the fault to slip.

Results of this type of SMTI analysis can be useful in correlating seismicity to known geological structures and provide some insights into the source mechanism and fault-slip direction; however, they often show a very complex picture with a wide range of source mechanisms. In some cases, meaningful information regarding stress orientation and rotation over time and mining can often be extracted from these results based on event selection, event quality and time spans when analysed in conjunction with mining geometries.

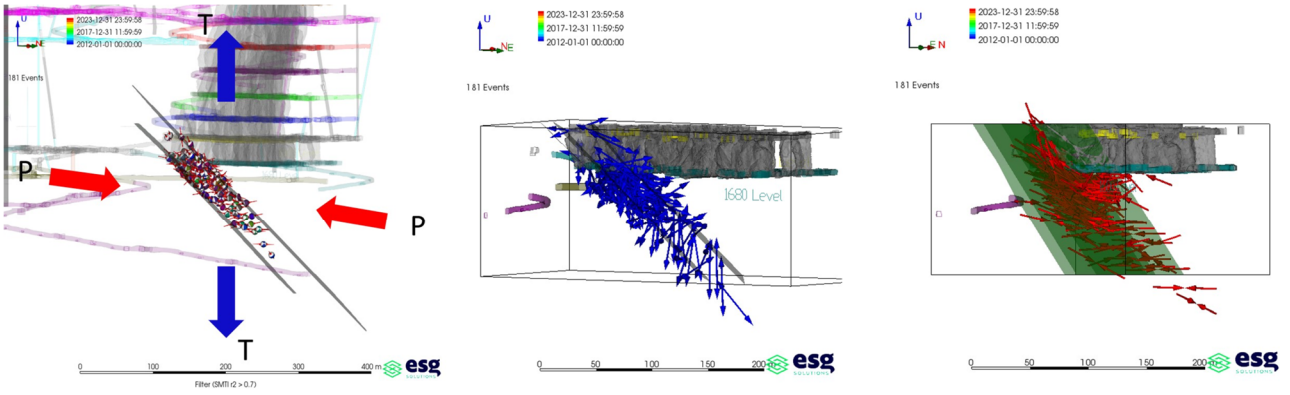

(a) (b) (c)

Figure 11 SMTI solution for 1680 West fault zone. Events greater than MW0.0 between 2012 and 2023 were analysed (ESG Solutions 2024). (a) Rotated view showing SMTI solutions, stopes, and fault model; (b) Tension (T) axes; (c) Pressure (P) axes

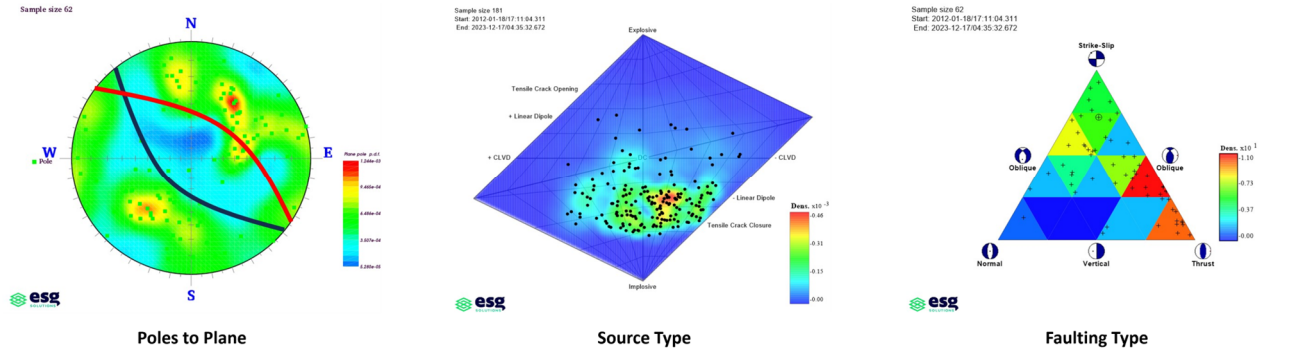

(a) (b) (c)

Figure 12 SMTI results for events with less than 30% volumetric failure component (ESG Solutions 2024). (a) Poles-to-plane plot. The failure plane shown by the red line is consistent with the 1680 West fault zone; (b) Source type showing dominant shear with closure mechanism; (c) Faulting type showing oblique thrust movement

6 Stress-channelling mechanism

A relatively consistent observation at NRS Mine is that the zone of weakness defining the persistent faults is sufficiently thick to cause stress channelling between the stoping front and the fault zone. Typical observations in diamond drillcore include low rock quality designation (RQD) and core recoveries near more-significant faults and a zone of increased jointing and alteration. Similar observations are made underground when tunnels intersect the faults. Although the zone of influences varies between faults and along different portions of the same faults, it is usually observed for several metres on either side of the thin gouge zone defining the fault.

In rock mechanics, several modelling techniques and methodologies have been used in the past decade to assess rockburst hazards in deep underground mines (Wang et al. 2021). The faults can be represented implicitly (low RQD zone, ubiquitous joints) or explicitly (interface) within continuum numerical models. Interfaces are typically used when sliding or separation along the geological structures is being analysed. A low RQD zone along the fault thickness can be used to capture a zone of weakness. The ubiquitous joint approach simulates a zone of preferential weakness in the numerical model along the fault orientation. Fault representation in the numerical models is almost always a simplified single plane approximation of the

true geological structure (Kim & Larson 2019). In reality, the faults are much more complex due to inherent thickness variation, gouge, geometrical anomalies, and asperities.

A FLAC3D mine-scale model employing the IMASS (ITASCA 2023) constitutive model is routinely used at the NRS Mine to understand stress-related hazards and to evaluate and support tactical and strategic mining decisions. For seismically active faults, a ubiquitous joint zone (1.5–2 m) along the fault interpretation is used to simulate the stress-channelling mechanism and evaluate the stress. An example of the modelling simulations is provided in Figures 13 and 14, showing the deviatoric stress concentrations, recorded seismicity, and accumulated plastic shear strain in the fault zone at the end of 2018 Q1 and Q2, respectively. The seismic data is clipped by 5 m on either side of the stress or fault plane.

High deviatoric stress concentration between the mining front on the 1680 level and the fault zone is evident, highlighting the stress-channelling mechanism (Figure 13a). The irregular fracture zone around the stoping front is due to the double abutment effect between the mining front, the 1660 sill above and the 1680 West fault zone. Observed seismicity is from the crosscut development for the next end slicing stope (Figure 13b) and correlated well with the stress state around the crosscut. The shear strain on the fault plane shows the areal extent of the mobilised fault zone from previous mining.

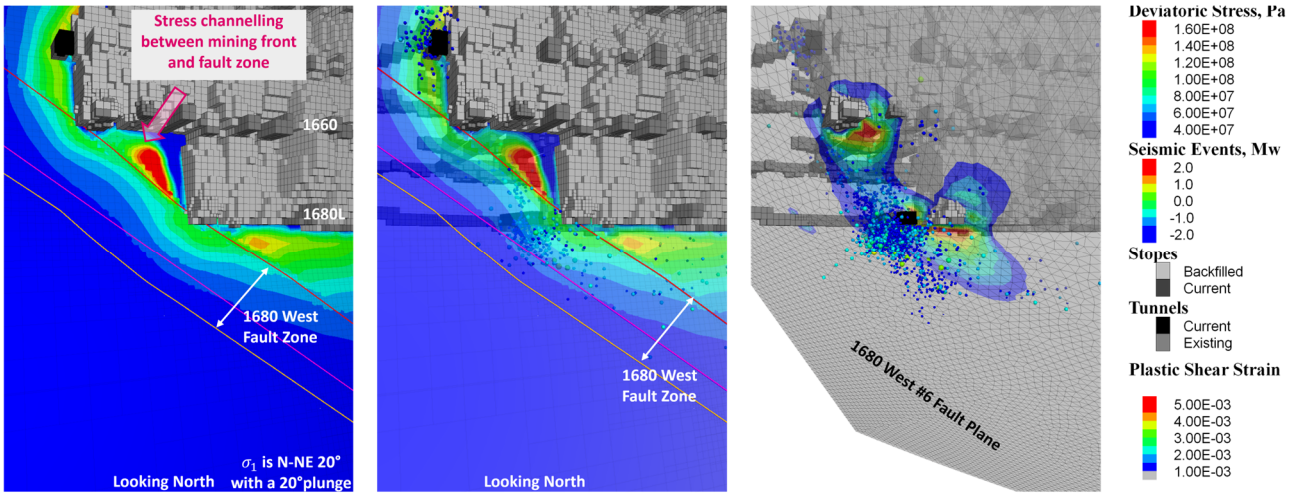

(a) (b) (c)

Figure 13 Mining step at the end of 2018 Q1 showing the stress-channelling mechanism between the mining front and the fault zone. (a) Deviatoric stress concentration; (b) Deviatoric stress overlayed with recorded seismicity; (c) Plastic shear strain in the fault zone overlayed with recorded seismicity

Figure 14 shows the next stope in the sequence mined through the stress-trapped pillar. The pillar between the mining front and the fault zone is fully yielded and/or stress shadowed (Figure 14a). The stope extraction resulted in stress pushing into the fault zone and a relatively higher seismic response (Figure 14b). A considerable change in the shear strain on the 1680 West #6 fault plane can be seen, suggesting a larger area of the fault being mobilised with the stope extraction (Figure 14c).

The modelling methodology presented can simulate the stress-channelling mechanism reasonably well and can be used to comparatively evaluate fault-slip risk associated with different strategic mining decisions, such as mining toward or away from a seismically active fault, and it can inform and support tactical decisions regarding ground support selection. However, faults remain challenging to simulate accurately in continuum numerical models, as the true strength and zone of influence of different faults and strength variability within the same fault cannot be accurately determined.

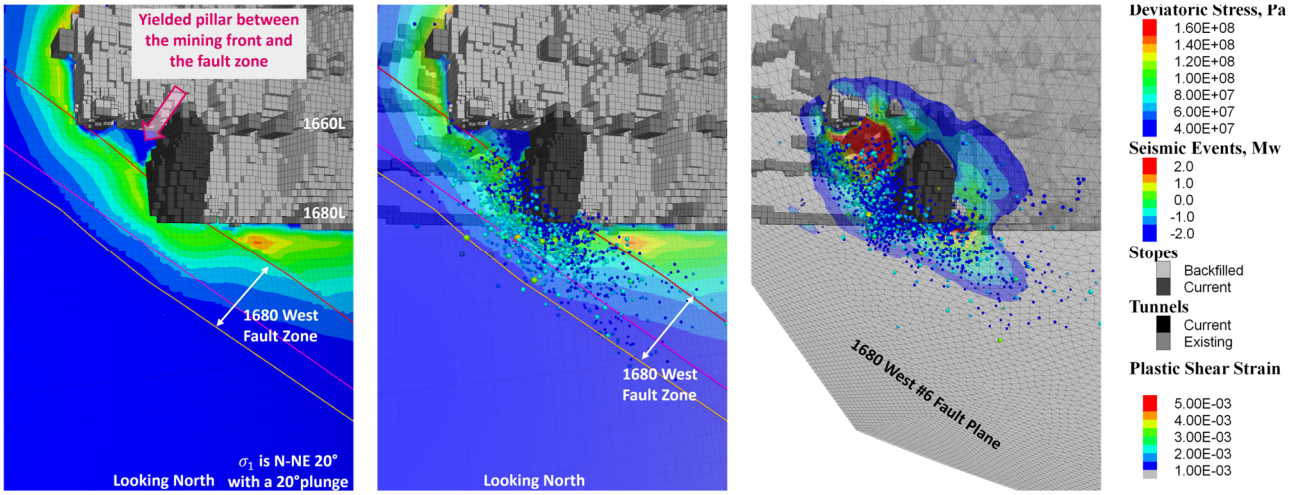

Figure 14 Mining step at the end of 2018 Q2 showing pillar between mining front and fault yielded and increased stress concentration within the fault zone. (a) Deviatoric stress concentration; (b) Deviatoric stress overlayed with recorded seismicity; (c) Plastic shear strain in the fault zone overlayed with recorded seismicity

7 Conclusion

Fault-slip seismicity is a major focus of the seismic risk management plan at NRS Mine. The fault-slip mechanism has been responsible for most of the mines' large seismic events and intense seismic episodes (periods of abnormally high activity). The structural fabric at the mine consists of several parallel north–south and oblique structures, and the strategic approach of mining away from seismically active faults is not always feasible, considering the fact that the seismic behaviour of fault zones evolves and changes as mining progresses. Mining away from one fault generally would have led to mining towards another fault in the NRS case. Several of these intense seismic responses at the mine were due to the stress-channelling mechanism, with stress being focused in the portion of the rock mass between the fault zone and the mined-out stopes. Numerical modelling can successfully capture this mechanism, enabling the mine to evaluate future mine sequencing decisions and/or implement proactive risk-mitigation strategies. Analysis of the seismic data allows the NRS Mine to calibrate these models and gain confidence in their validity.

Extended and widespread re-entry protocols, enhanced ground support, preventative maintenance of existing ground support, and remotely operated equipment are all examples of reducing exposure and risk to damaging seismic events. There is a clear trend of increasing risk that the mine-scale geological structures may become activated as the overall extraction rate of the mine increases across all levels and in all directions, and larger parts of the rock mass experience stress changes. The faults that go obliquely through the orebody have portions of the structure that are always located in an abutment. Some of the mines' transversely oriented steeply dipping faults have had the risk profile change over time in a different way. The seismic or fault-slip risk increases with mining, especially when converging mining fronts occur, and then can subsequently decrease as the mining front passes through the structure. Both increased driving stress and, in other areas, clamping stress occur in the mines' sill extraction and high-stress abutments. A sudden release of clamping or an increase in the shear stress can lead to larger-scale fault-slip events.

Even though the modelling methodology presented in this paper can be used to evaluate various mining strategies in high-risk areas around the seismically active faults, there is still significant work to be done to accurately represent and model geological faults in numerical models that can be used to drive key operational decisions. One of the main difficulties encountered while tracking mining-induced seismicity along fault zones is the fact that faults creep, emit small-magnitude seismic activities, and occasionally slip, leading to larger-magnitude seismic events. There is rarely enough detailed knowledge of the faults' strength variation and asperity geometry. Seismic events locating close to a fault zone may result from rock fracturing near the fault due to the induced loads caused by the fault movement. So, for example, comparing

numerically modelled parameters such as cumulative plastic strain along a fault might not directly correlate to observed seismicity.

Emerging technologies such as fibre optic sensing (Furlong & Anderson 2022; Dande et al. 2024) will allow relatively cost-effective sensors that can capture strain, seismic arrival times, and temperature changes to be deployed in mining environments. For example, a well-known observation at NRS mine is water seepage through the fault zones (mining process water from backfilling or drilling). Temperature tracking could track this, and strain monitoring from the fibre could capture some of the aseismic fault creep. Other monitoring techniques, such as three-dimensional lidar scanning, can improve deformation tracking in existing openings, albeit the main deformation mechanism in highly competent rock mass is usually rock mass bulking between tendons ('screen bagging'). Conventional instruments, such as extensometers installed across the fault zone, can be used to capture deformation over time. However, determining the direction of monitoring with respect to the fault slip remains challenging. Widespread use of geophysical techniques, such as seismic imaging, may offer potential for improved fault-geometry models. Seismic monitoring has proven to be an essential tool for deep and high-stress mining, especially when fault-slip seismicity is a major contributor.

Acknowledgement

The continued support of Sudbury Integrated Nickel Operations Management is gratefully acknowledged. Present and past NRS geology and ground control team members, particularly Ed Deneka and Lloyd Howell, are also acknowledged. The partnership with the mines' seismic system provider (ESG Solutions) and the use of the mXrap (Harris & Wesseloo 2015) software package (Australian Centre for Geomechanics) are also key components of this work.

References

Dande, S, Forbes, E, Butler, T, Hall, A, Simser, B, Chauvet, R & Cherubini, A, 2024, 'Utilising distributed acoustic sensing for monitoring rock mass stress conditions in underground mining: a case study', in P Andrieux & D Cumming-Potvin (eds), *Deep Mining 2024: Proceedings of the 10th International Conference on Deep and High Stress Mining*, Australian Centre for Geomechanics, Perth, pp. 375–390.

ESG Solutions, 2021, *Nickel Rim SMTI and Stress Inversion – June 4, 2020 Event Analysis*, internal report.

ESG Solutions, 2022, *Nickel Rim SMTI and Stress Inversion – July 8, 2021 Event Analysis*, internal report

ESG Solutions, 2024, *Nickel Rim SMTI Analysis of Deep Events from 2012 to 2023*, internal report

Furlong, J & Anderson, Z 2022, 'Distributed acoustic sensing/distributed strain sensing technology and its applications for block cave progress monitoring, rock mass preconditioning, and imagining', in Y Potvin (ed.), *Caving 2022: Proceedings of the Fifth International Conference on Block and Sublevel Caving*, Australian Centre for Geomechanics, Perth, pp. 991–1006, https://doi.org/10.36487/ACG_repo/2205_68

Harris, PH & Wesseloo, J 2015, *mXrap*, version 5, computer software, Australian Centre for Geomechanics, The University of Western Australia, Perth, https://www.mxrap.com

ITASCA 2023, *FLAC3D – Fast Lagrangian Analysis of Continua in Three-Dimensions*, version 9, computer software.

Jalbout, A & Simser, B 2014, 'Rock mechanics tools for mining in high stress ground conditions at Nickel Rim South Mine', in M Hudyma & Y Potvin (eds), *Deep Mining 2014: Proceedings of the Seventh International Conference on Deep and High Stress Mining*, Australian Centre for Geomechanics, Perth, pp. 189–208, https://doi.org/10.36487/ACG_rep/1410_11_Jalbout

Kim, B & Larson, MK 2019, 'Development of a fault-rupture environment in 3D: a numerical tool for examining the mechanical impact of a fault on underground excavations', *International Journal of Mining Science and Technology*, vol. 29, pp. 105–111.

Mendecki, A, van Aswegen, G & Mountfort, P 1999, 'A guide to routine seismic monitoring in mines', in AJ Jager & JA Ryder (eds), *A Handbook on Rock Engineering Practice for Tabular Hard Rock Mines,* Safety in Mines Research Advisory Committee to the Department of Minerals and Energy of South Africa.

Morkel, IG, Wesseloo, J & Potvin, Y 2019, 'The validity of Es/Ep as a source parameter in mining seismology', in W Joughin (ed.), *Deep Mining 2019: Proceedings of the Ninth International Conference on Deep and High Stress Mining*, The Southern African Institute of Mining and Metallurgy, Johannesburg, pp. 385–398, https://doi.org/10.36487/ACG_rep/1952_29_Morkel

Saleh, R, Milkereit, B & Liu, Q 2015, 'Simulation of seismic wave propagation in a deep mine', *Proceedings of GeoConvention*.

Saleh, R & Milkereit, B 2014, 'A modelling study of broadband seismic wave propagation in a deep mine', *76th EAGE Conference and Exhibition 2014*, European Association of Geoscientists & Engineers, Bunnik.

Simser, B 2019, 'Rockburst management in Canadian hard rock mines', *Journal of Rock Mechanics and Geotechnical Engineering*, vol. 11, no. 5, pp. 1036–1043.

Simser, B 2022, 'Applied seismic monitoring for decision making in deep hard rock mines', *Proceedings of RaSim10: Rockbursts and Seismicity in Mines*, Society for Mining, Metallurgy & Exploration, Englewood.

Simser, B & Butler, T 2022, 'The value of recording small mining induced microseismic events with examples from Glencore's Nickel Rim South Mine', *Proceedings of RaSim10: Rockbursts and Seismicity in Mines*, Society for Mining, Metallurgy & Exploration, Englewood.

van Aswegen, G & Butler, AG 1993, 'Applications of quantitative seismology in South African gold mines', in RP Young (ed.), *Proceedings of the 3rd International Symposium on Rockbursts and Seismicity in Mines*, A.A. Balkema, Rotterdam, pp. 261–266.

van Aswegen, G, 2013, 'Forensic rock mechanics, Ortlepp shears and other mining induced structures', *Proceedings of the Eighth International Symposium on Rockburst and Seismicity in Mines Proceedings*.

Wang, J, Apel, DB, Pu, Y, Hall, R, Wei, C & Sepehri, M, 2021. 'Numerical modeling for rockbursts: a state-of-the-art review', *Journal of Rock Mechanics and Geotechnical Engineering*, vol. 13, no. 2, pp. 457–478.

Yadav, P, 2024 'Geomechanical evolution of the Nickel Rim South Mine', in P Andrieux & D Cumming-Potvin (eds), *Deep Mining 2024: Proceedings of the 10th International Conference on Deep and High Stress Mining*, Australian Centre for Geomechanics, Perth, pp. 61–84